Neurovascular structures in human vastus lateralis muscle and the ideal biopsy site

SCHOLARONE™
Manuscripts

Neurovascular structures in human vastus lateralis muscle and the ideal biopsy site

Running title: human vastus lateralis biopsy site

Authors:

Xin Chen[1], Steve Abbey[2], Adam Bharmal[3], Sophie Harris[4], Edward Hudson[5], Lisa Krinner[6], Emma Langan[7], Alex Maling[8], Jagdip Nijran[9], Hannah Street[10], Charlotte Wooley[11], and Rudolf Billeter[12*]

Current affiliations:

1: School of Computer Science, University of Nottingham, Nottingham UK

2: University Hospital Coventry & Warwickshire - UK Foundation Programme

3: School of Medicine, University of Nottingham, Nottingham UK

4: NHS Lothian, South East Scotland Deanery, NHS Scotland UK

5: UK Foundation Programme, NHS UK

6: Department of Public Health Sciences, College of Health and Human Services, University of North Carolina at Charlotte, USA

7: Royal Derby Hospital, Derbyshire - UK Foundation Programme

8: Auckland City Hospital, Auckland District Health Board, New Zealand

9: Wexham Park Hospital, Frimley Health Foundation Trust UK

10 Wythenshawe Hospital, South Manchester NHS Trust UK

11: Ashford and St Peter's Hospitals, NHS Trust, UK

12: School of Life Sciences, University of Nottingham, Nottingham UK

1

*: corresponding Author

Address: School of Life Sciences

                University of Nottingham

                Queen's Medical Centre

                Nottingham

                NG7 2UH

                UK

Tel. ++44 115 823 0168

Fax ++44 115 823 0142

e-mail rudolf.billeter-clark@nottingham.ac.uk

2

Abstract

A density model of neurovascular structures was generated from 28 human vastus lateralis muscles isolated from embalmed cadavers. The intramuscular portion of arteries, veins and nerves was dissected, traced on transparencies and digitised before adjustment to an average muscle shape using Procrustes analysis to generate density distributions for the relative positions of these structures.

The course of arteries, veins and nerves was highly variable between individual muscles. Nevertheless, a zone of lower average neurovascular density was found between the tributaries from the lateral circumflex femoral and the deep femoral arteries. While the area with the lowest density was covered by the iliotibial tract and would therefore not be suitable for biopsies, another low-density area was located in the distal portion of vastus lateralis. This was just anterior to the iliotibial tract, in a zone that has been described as a good needle biopsy site. The reported complication rates of needle biopsies (0.1-4%) are in the range of expectations when simulated based on this model.

It is concluded that the optimal human vastus lateralis biopsy site is in the distal portion of the muscle, between ½ and ¾ of the length from the greater trochanter to the lateral epicondyle, just anterior to the iliotibial band.

Introduction

The muscle biopsy is a routine procedure to obtain human muscle tissue for research and diagnostic purposes. Although small, biopsies provide representative samples for many muscle phenotypes, and much of the current detailed knowledge regarding human acute and chronic muscle adaptation to exercise has been obtained from biopsies. They are generally well tolerated but a small risk remains[1].

To a majority, muscle biopsies are obtained using the Bergström needle with or without modification [2,3]. When the procedure is performed with suction, samples of 200 mg or more can be obtained [4], which is sufficient for most modern analyses.

Micro-needle biopsies [5] are a less traumatic alternative to the Bergström needle, with a yield of about 20 mg or less. The conchotome procedure provides tissue yields comparable to the Bergström needle[6]. Open biopsies – which are preferred in the diagnosis of some forms of myositis - can provide greater than 1000 mg of muscle tissue [1] but can be more traumatic. Dorph et al.[7] however reported comparable myositis detection rates when comparing open biopsies with repeated conchotome biopsies.

The needle biopsy procedure has been described in a number of publications, possibly the most detailed in Shanely et al.[3].

In short, the skin is treated with antiseptic before the skin and underlying fascia are anaesthesised local to the biopsy site. This allows a painless incision through skin and fascia through which the needle is inserted to harvest muscle tissue. Pressure is applied onto the biopsy site for about 10-15 minutes to reduce bleeding since micro-vasculature is inevitably cut. Either stitches [4], skin compatible tape [7] or surgical adhesive [3] has been used to close the incision site.

The needle muscle biopsy procedure is normally done "blind", with no view of the cutting site. There is a very rare chance that a larger vessel can be cut, resulting inbleeding to an extent that cannot readily be stopped by thecompression that is routinely applied after a biopsy. This can result in haematoma, which has been described as a principle complication of muscle biopsies [8]. While the

4

supply of blood to the human muscles is known in great detail, information about the course of blood vessels within our muscles is scant.

This study aims to provide novel insight on this topic for the human m. vastus lateralis, from which most muscle biopsies are obtained. It is the largest portion of the quadriceps femoris in the majority of people [9] and can be readily accessed through the skin. In addition, it is not repeatedly subjected to outside pressure, as is the case with the gluteus maximus, for example, which helps in recovery from biopsy trauma. No major nerves or blood vessels run through or close to the m. vastus lateralis and there is a large body of data on this muscle for comparison.

The vastus lateralis is also used for muscle / skin flaps [10], for example in oral reconstruction, remarkably without major impact on the patients' locomotor abilities.

The vastus lateralis proximal attachment is at the greater trochanter (with variable contacts in the adjacent part of the femur), from which the large, thin proximal aponeurosis covers a substantial part of the muscle's surface [11]. From this aponeurosis, the bulk of the muscle's fascicles connect to the distal (deep) aponeurosis, which converges into the quadriceps tendon. It is essentially a unipennate muscle. Vastus lateralis is closely linked to the underlying vastus intermedius. In their posterior part, the two muscles are fused to a variable extent[12].

The blood supply to and from the vastus lateralis is via branches of the lateral circumflex femoral artery and vein, mainly from the descending branch [10] and branches from the deep femoral artery which perforate the lateral intermuscular septum [13–15]. Branches from these main vessels form an anastomosing[15,16] network. Most distally, the geniculate network contributes as well [16].

Femoral nerve branches innervate vastus lateralis. In many individuals, they split before entering the muscle in its anterior proximal portion[11,17]. Within the muscle, nerve branches often run in septa next to vessels.

By providing a probability distribution of the main vessels and nerves within the vastus lateralis, this study aims to identify those biopsy sites which have the lowest chance of complication on the one

5

hand and to assess the inter-individual variability of the intra-muscular nerve and vessel patterns on the other. The latter is potentially important for the interpretation of results from small muscle biopsies. Larger vessels run in larger septa which can contribute a disproportional amount of connective tissue to bulk measurements performed on such biopsies.

6

Methods

Donors

Intramuscular neurovascular trees in this study were obtained from 28 human vasti laterales, either from the right (13) or the left (15) thigh. Their donors (11 females, 17 males) were White Caucasian with a median age of 87.5 years (60-97). The cadavers had been embalmed in a solution of 81.2% ethanol, 4.5% methanol, 3% phenol and 1.4% formaldehyde.

Arteries, veins and nerves were prepared by dissection and traced onto transparencies (see below, Figure 1). After adjustment to a common shape as described below, they could be superimposed to generate 2-dimensional density maps which are shown in the Supporting Figures S2 for the whole cohort and S4 A and S5 A for female and male vasti separately.

In order to get an estimate of volume density, 3D models were generated from another comparable cohort of 18 donors and combined to an average vastus lateralis volume (Supporting Figures S3 for the whole of this cohort and S4 B and S5 B for muscles from female and male donors, respectively). Vasti laterales were obtained from the right (6) and left (12) legs of 10 male and 8 female White Caucasians with a median age of 84 years (65-98).

The donor of the vastus lateralis shown as a 3D reconstruction in Figure 4 and Supporting Figures S8 and S9 was a 78-year-old male with a height of 185 cm.

All donors died of natural causes, and largely due to respiratory or circulatory complications. None had known pathology of the musculature.
All had given consent to the use of their body for Anatomical examination, education, training and research at the University of Nottingham in accordance with the Human Tissue Act 2004.

Isolation of vastus lateralis

The partially freed vastus lateralis was lifted from its *in situ* position, working from a cut just past the distal end of the muscle. Anteriorly, it was clearly separated from vastus intermedius by the deep aponeurosis. Posteriorly, the two muscles were fused to a variable extent as previously described [12]. Blunt separation was used to reflect the vastus lateralis from the vastus intermedius as far as possible. In this arrangement, vastus lateralis fascicles ran parallel to the axis of the rectus femoris while vastus intermedius fascicles were oblique, which allowed us to separate them by sharp dissection. The final step was the sharp separation of the vastus lateralis origin from the greater trochanter. No vastus lateralis was found to have an additional origin along the linea aspera as described in some Anatomy textbooks.

Artery, vein and nerve dissection and tracing

Arteries, veins and nerves were dissected from their entry site into the vastus lateralis until they were not visible through a magnifying glass (Daylight, 1.75x), ie. about 0.5 mm thickness. This required some cutting and removal of fascicles.

To generate tracings from the dissected vessels and nerves, the muscle was laid flat (Figure 1A) and the prepared arteries, veins and nerves were painted with nail polish (Figure 1B) to enhance visibility. An A3 acetate sheet was pinned onto the vastus lateralis and the muscle outline, arteries, veins and nerves was carefully traced using felt tipped pens. This was subsequently scanned to generate a .jpeg file with a pixel size of 0.035x0.035 cm (Figure 1C). The tracings from the right leg (for example muscles C, D and H in Figure 2) were mirrored to be consistent with the left leg.

The tracings formed the basis for the subsequent analysis which was performed using the Fiji bundle of imageJ [18] and Matlab (The Mathworks Inc., Natick, Massachusetts, USA).

Estimate of artery and vein trace length and the proportion of arteries associated with veins

A majority of arteries were accompanied by venae comitantes, often on each side (Figures 1 and 2). A rough length estimate of the dissectable intramuscular arteries and veins and their proportion of juxtaposition was obtained with imageJ.

Both the arterial and venous trees (Supporting Figure S1 C, F) were transformed into black binary skeletons of 1-pixel width on a white background (Supporting Figure S1 D, G). The muscle, delineated by its outline (Supporting Figure S1 A), was rendered black on a white background (Supporting Figure S1 B). Adding the black muscle shape to a vein or arterial skeleton yielded the intramuscular proportion of that skeleton (Supporting Figure S1 E, H). Given that it was one pixel in diameter, its length could be determined as the total black pixel area. The values in Table 1 represent the tree lengths in pixels multiplied by the pixel diameter (0.035cm).

To estimate the proportion of arteries in proximity to veins, the venous tree was expanded to a zone of 3mm on either side of the skeleton trace. This image was then inverted (Supporting Figure S1 I) and added to the intra-muscular skeleton portion of the arteries, leaving only those arterial traces that were more than 3 mm away from the centre of a vein (Supporting Figure S1 J).

The same approach was used to determine the length of the dissected nerves and their proportions neighbouring a vessel. The proportion of "free" nerves not neighbouring a vessel was determined by adding the white, thickened venous (Supporting Figure S1 I) and arterial trees (not shown) to the black nerve trace skeleton.

Alignment of arteries, veins and nerves for density estimation

The tracings in Figures 1 and 2 illustrate the inter-individual variability of vastus lateralis shapes and neurovascular structures. To determine the local vessel densities, they were adjusted to a common muscle shape.

For 2D density estimates, the tracings were aligned to a common reference coordinate using Procrustes analysis [19]. Firstly, one of the muscle circumferences was randomly selected as an initial reference shape. Then all the muscle circumferences were adjusted to the reference mean shape by a

9

four-step iterative process. In step 1, the circumferences were aligned at their centroids. For step 2, the corresponding contour points between a given circumference and the reference shape were determined based on the minimum Euclidean distance between them. This was done for all circumferences. The reference shape was then updated to the mean coordinates of all corresponding points in step 3. In step 4, each of the circumferences was scaled and rotated (rigid transformation) to this new reference shape based on the corresponding points. Step 1 to step 4 were iterated until the rotation and scale parameters in step 4 were unchanged, resulting in a final mean reference shape. Each of the artery, vein and nerve maps was then transformed to the final reference coordinate based on the estimated scale and rotation parameters. They could then be superimposed, resulting in the images of Supporting Figures S2, S4 A and S5 A. The mean shape of the circumferences is shown as a red contour in Figures 3 and Supporting Figures S 6 and S7.

These calculations were done using a custom-written Matlab program which can be obtained from the corresponding author upon request.

Estimation of volumetric density

The densities shown in Supporting Figures S2, S4 A and S5 A do not take depth into consideration. Since depth information could not be obtained from the dissected muscles, the vasti laterales from another, comparable cohort of 18 donors (10 males and 8 females, see "*Donors*") were used to generate averaged 3D vastus lateralis models.

For this, 3D point clouds from each of the 18 muscles were produced with a Vectra 3d H1 camera and converted to depth maps (in mm). The contour of each circumference was extracted and aligned, again using the Procrustes analysis, to the 2D final reference mean shape. An A B-spline deformable image registration method [20] was subsequently applied to refine the depth map alignment. Finally, average 3D vastus lateralis models were generated (Supporting Figures S3, S4 B and S5 B) based on the alignment of the depth maps to the relevant reference shapes. These 3D models were combined with the previously calculated 2D vessel and nerve density maps to model the volumetric vessel and

10

nerve densities shown in Figure 3 and Supporting Figures S6 and S7.

These operations were also done with custom-written Matlab scripts which can be obtained from the corresponding author upon request.

3d reconstruction of a human vastus lateralis surface

Figure 4 shows the combined volume density map of Figure 3 applied to the vastus lateralis surface of a 3D reconstruction from the anterior and lateral portion of a human thigh.

The 3D thigh surface was generated by photogrammetry from a 78-year-old male donor. One hundred and thirty-six overlapping colour images were taken with a digital camera (Nikon D50100), systematically surrounding the thigh under diffuse lighting. VisualSFM [21,22] was used to generate a 3D point cloud from these images. It was imported into Meshlab [23] and cleaned from spurious points before turned into a triangular mesh using the program's Poisson mesh generator.

From this surface mesh, the vastus lateralis muscle belly was isolated and the combined volume density map of Figure 3 was fitted to it, Procrustes adjustment was employed so that it could be applied as a raster to the isolated vastus surface in Matlab. The "rastered" vastus surface was then fitted back onto the thigh model.

To link this 3D model to palpable structures, a line was drawn between the greater trochanter and the lateral base of the patella in Meshlab by hand. The same was done for the iliotibial tract and the biopsy sites described in the literature (Figure 4 B and its 3D version S9 in the supporting material). The borders of the iliotibial tract were estimated from Flato et al. [24].

The thigh had position markers placed in the form of screws, indicating the anterior superior iliac spine, top of the greater trochanter, lateral epicondyle and the middle of the patella. These were used to orient and scale this 3D model to the measures of the original thigh in the virtual space of Meshlab, which allowed for direct comparison with the parameters of recommended biopsy sites from the literature.

11

Statistics

Student's t-tests were used to judge the difference between male and female parameters shown in

Table 1. These were run in SPSS version 23 (IBM Corp. Released 2015. IBM SPSS Statistics for

Windows, Version 23.0. Armonk, NY, USA: IBM Corp.).

1
2
3
4
5
6
7
8
9
10
11
12
13
14
15
16
17
18
19
20
21
22
23
24
25
26
27
28
29
30
31
32
33
34
35
36
37
38
39
40
41
42
43
44
45
46
47
48
49
50
51
52
53
54
55
56
57
58
59
60

Results:

Vessel and nerve distribution in individual vasti laterales

Figure 2 shows representative tracings of arteries, veins and nerves from 8 of the 28 vastus lateralis

muscles analysed. It illustrates the large inter-individual variability in these structures.

Table 1 summarises the length of the traces from female and male vastus lateralis muscles and both

sets of data combined.

Significant differences between the genders was found for muscle length and – accordingly- the intra-

muscular length of the traced arteries, veins and nerves

About 80% of the isolated arteries were accompanied by at least one vena comitans (proportion of

arteries accompanied by veins in Table 1). They often formed vein-artery-vein triplets, as illustrated

in Figure 1 A and Figure 2 A, B, E and F. The total length of the dissected veins was therefore more

than the arteries (~113 vs. 77 cm). The proportion of arteries associated with veins was significantly

greater in vasti from females (~85%) compared to males (~77%, Table 1).

Nerves were found to be within 3 mm of a vessel for 67% of its detectable length (proportion of

nerves neighbouring a vessel in Table 1). No difference in nerve-vessel association between male and

female muscles was found.

In most of the analysed muscles, the main blood supply (~73%, proportion of arteries/veins from

branches of LCFA/LCFV in Table 1) was from and to branches of the lateral circumflex femoral

artery and vein, indicated by arrowheads ① in Figure 2 A to D. A minor portion (~27%) was from and

to branches arising from the deep femoral artery and vein (arrowheads ② in Figure 2 A to D).

Only two of the 28 vasti laterales had >50% of their arterial blood supply from the main branch of the

deep femoral artery. An example is muscle G in Figure 2, in which no descending branch of the

lateral circumflex artery was found but the vein was present. In 4 muscles, all the dissectable arteries

were branches of the LCFA and no vessels from and to the deep femoral artery/vein network were

found. An example is muscle F in Figure 2.

Anastomoses between the lateral circumflex femoral and the deep femoral vessels could be traced in

13

12 muscles. They were to a majority venous. Examples are indicated by arrowheads ③ in Figure 2 B, C and D.

Most of the vessels entered the vastus lateralis at its anterior or posterior margin. Since the focus of this study was the intra-muscular neuro-vasculature, we did not systematically follow the arteries, veins or nerves back to their origin.

In 11 muscles, we found vessels entering the vastus lateralis on its deep aspect, most of them as branches from the underlying vastus intermedius circulation. Examples are indicated by arrowheads ④ in Figure 2 A, B and H. In 4 muscles, arteries entered from the surface of the femur deep in the very proximal part of the muscle, as indicated by arrowhead ⑤ in Figure 2 E.

Nerves entering the vastus lateralis from its posterior or deep aspects were found in 5 of the 28 muscles. Arrowhead ⑥ in Figure 2 E points to an example. These were branches that probably travelled through vastus intermedius.

Model of volumetric densities

The volumetric density of arteries, veins and nerves from all 28 dissected vasti laterales is shown in Figure 3. It combines the information of the superimposed 2D tracings shown in Supporting Figure S2 with the depth information of an average 3D vastus lateralis shape that was generated from a comparable cohort of donors shown in Supporting Figure S3.

We could not detect any overt differences in distributions of vessels or nerves between vasti from male and female donors using the same approach. The volumetric density maps are shown in Supporting Figures S6 and S7, the corresponding 2D density and height maps are shown in Supporting Figures S4 and S5. This led us to concentrate the analysis on the data from all 28 dissected muscles in order to obtain a best refined model.

The volumetric densities in Figure 3 show a middle zone of lower vein and artery density, with nerves being less dense posterior to that line. The colour scale is adjusted to reflect the likelihood of a

14

cylinder with 4 mm diameter and 15 mm length incorporating a mapped neurovascular structure. This cylinder is an approximation of a 200 mg biopsy obtained with a Bergström needle with suction. The zone with the lowest density of dissectable neurovascular structures is outlined in white. Figure 4 indicates that it lies in an area covered by the iliotibial tract.

Figure 4 A illustrates the density map in the context of the palpable landmarks on the thigh. It shows screenshots from a 3D reconstruction of an *in situ* m. vastus lateralis from a 78-year old male donor, with the combined neurovascular volume density map of Figure 3 adapted to its surface. The Supporting Figure S8 contains the corresponding 3D model as 3D-pdf file. A red line has been drawn between the greater trochanter and the lateral part of the patellar base. Light green indicates a projection of the iliotibial band onto the model, broadened in the proximal part by the tendon of the tensor fasciae latae merging into it.

Figure 4 B shows this 3D neurovascular density model with some of the biopsy sites described in the literature (Table 2) superimposed.

The zone with the lowest combined volume density, outlined in white in as Figure 3, is mostly covered by the iliotibial tract and the tensor fasciae latae tendon merging into it. This renders it unsuitable for a needle biopsy. Pointing distally from the middle of the muscle, there is another zone of low neurovascular density, about 1 cm wide and 8 cm long, just anterior to the iliotibial band, which would be most suitable for the collection of a needle biopsy according to this model. This is the zone recommended by Tarnopolsky et al.[1] as indicated in Figure 4 B by the purple colour.

Except for the very middle, there is an area with mostly low to medium neurovascular density. This stretches between half and three quarters of the distance between the greater trochanter and the lateral epicondyle, bordered by a line from the greater trochanter to the lateral base of the patella anteriorly and the iliotibial band posteriorly. This seems to be suitable for needle biopsies according to our model. The area anterior to the trochanter-lateral base of patella-line has the highest density of such structures. The most distal quarter of the muscle has very low density, but is normally too thin, as indicated in the average height map in Supporting Figure S3.

15

Discussion:

Optimal needle biopsy site

The area with the lowest neurovascular density in the model generated in this study (surrounded by a white line in Figures 3 and 4) is covered by the proximal portion of the iliotibial tract and the tendon of the tensor fasciae latae. Another area of low neurovascular density identified is located just anterior to the iliotibial band, stretching distally from the middle of the muscle to about 75% of its length, about 1 cm wide. An area between the middle of the vastus lateralis muscle and about 75% of its length distally, bordered anteriorly by a line stretching from the greater trochanter to the lateral base of the patella and posteriorly by the iliotibial tract had mostly medium to low neurovascular density. This is an area that many groups recommend to obtain muscle biopsies from, as discussed below.

It is widely accepted that needle biopsies are well tolerated and the rate of complications is rare[28–30]. While most subjects will feel dull, light pain at the biopsy site, this is no deterrent to performing exercise shortly thereafter. In some studies (e.g. [31]), biopsies have been obtained during exercise without problems. The frequency of complications is low, between 0.1% and 4%, as indicated in table 3. The majority (bleeds, pain) relate to the vascular system. The volume density map in Figure 3 indicates that the risk of damaging a larger vessel or nerve is 2-4 times greater if biopsies are obtained anterior to the line between the trochanter and the lower base of the patella.

The published recommendations for a m. vastus lateralis biopsy site vary somewhat, as listed in Table 2. They correspond to differently coloured areas in Figures 4B and Supporting Figure S9. While the recommendations in [1] and [3]correspond to the purple painted zone of low neurovascular density in this study's model. the other sites recommended lie in that mid to distal zone that also has medium to low level density.

In Figures 3 and 4, densities were modelled as the probability that a cylinder of 4 mm diameter and 15 mm length (a biopsy of about 200 mg) would contact a dissectable neurovascular structure with the superimposed artery/vein and nerve tracings evenly distributed throughout the depth of the muscle.

16

Considering that the density distributions are based on 28 individual vasti laterales, the frequencies indicated in these figures should be divided by 28 to calculate the risk of damaging such a structure in a single biopsy. This yields approximate frequencies of ~0.3% for the low-density zone, ~0.8% in a zone with medium density and ~1.5% in a high frequency zone anterior to the trochanter to lateral base of patella line.

These frequencies correspond well to the rate of reported complications shown in Table 3, which is likely not to be attributable to chance. The tracings underlying the density maps show vessels and nerves dissected to ~ 0.5 mm diameter, which was the limit of free hand dissection. A vessel of this size would bleed if cut, likely until the compression normally applied to the thigh after a biopsy takes effect. This may lead to accumulation of sufficient blood to generate discolouring and/or pain lasting for several days.

The observation that the two publications which reported the lowest proportions of complications [1,3] recommended the distal zone with the lowest neurovascular density in this study supports this contention. It seems to be the optimal site for a biopsy in terms of possible complications.

We could not find a report of obvious intramuscular nerve damage by needle biopsies in vastus lateralis. Reported cases of localised numbness (e.g. 5 in 13626 biopsies [1]) were probably the consequence of injuries to branches of the lateral cutaneous femoral nerve, which run outside the fascia lata. The sensation recovers fully within a few months. The reports of deep pain lasting more than three days [1,26,27] are more likely a consequence of localised bleeding than sensory nerve injury. Given the density of the motor nerve branches within the vastus lateralis reported in this study, it would be expected that motor nerve injuries would occur at a somewhat lower frequency as the reported complications relating to vessel injuries listed in Table 3. Based on reports from anterolateral thigh flaps that required cutting a branch of the vastus lateralis motor nerve[32], which for a majority of the patients did not affect their mobility, it could be proposed that nerve injuries do happen in needle biopsy procedures, but are inconsequential to muscle function.

Inter-individual variability

The nerve and vessel tracings shown in Figure 2 illustrate the considerable inter-individual variability in shape and proportion of these neurovascular trees. This corresponds to reports of the use of anterolateral thigh flaps in reconstructive surgery [15,17]. It also compares to inter-individual differences found in vastus lateralis shape and its relationship to vastus intermedius and medialis [9,12] and gene expression[33].

In average, about 75% of the dissectable arteries and veins in this study were branches of the lateral circumflex femoral artery (LCFA in table 1) and 25% from (perforating) branches of the deep femoral artery, which corresponds to previous descriptions of the two arterial supplies [13,15]. Anastomoses could be traced between the two systems in 12 of the 28 muscles. Using latex injection into the lateral circumflex femoral artery and branches of the deep femoral artery, Grob et al. [14] showed extensive anastomoses between the lateral circumflex and deep femoral branches as well as lateral circumflex - lateral circumflex and deep-deep anastomoses. Most of these were missed in this study, probably because they were too delicate to be traced by free hand dissection. Given the good correspondence between reported complication rates (Table 3) and probabilities of damaging a vessel in this study, we suggest that these extensive anastomoses are mostly too small to represent a complication risk from a needle biopsy.

As indicated in the Results, the proportion of these two blood supplies varied widely between different vasti laterales. Of the 28 muscles analysed, 4 lacked traceable branches from the deep femoral artery, while two had more than 50% of their vessels from deep femoral artery branches. Thus, while the anastomoses ensure that trauma caused by a biopsy can be repaired locally and efficiently, variations in the blood supply make it difficult to reduce the chance of inducing a heamatoma to zero. Large to mid-size blood vessels can be a source of variability, especially when determining RNA, proteins or metabolites in bulk portions from a biopsy, due to different proportions between connective tissue and muscle fibres if the biopsy contains parts of a larger septum. We have, for example, found strong signals for ribosomal RNA and ribosomal proteins in in situ hybridisation

18

and immunohistochemistry experiments in some, but not all, arterioles / small arteries. This could influence total RNA yield, given that about 80% of bulk RNA is ribosomal.

Data, presented in Table 1 and Figures 1 and 2 indicate that most major intramuscular arteries (~81%) run with neighbouring, largely comitant veins and motor nerves (~67%) close to them. This fits the descriptions of [10,13], among many others, on the use of anterolateral thigh flaps, whose success depends on intact pedicles containing feeding arteries and veins and – in some cases - also nerves [17]. Inter -individual variability in the location of perforator arteries [34] poses a particular challenge for these procedures.

Limitations of the study

Given their advanced age, the muscles of our donors were inevitably in various stages of atrophy and subject to the known changes in the microvasculature that accompany the aging processes.
The model generated in this study is based on the dissectable MACRO-vasculature, however, whose pattern has been found to establish during early development and remain stable thereafter in rodents. This is thought to be the case for humans as well[35]. It is also the underlying assumption on which dissection-based anatomy teaching and surgical training is based world-wide, which is naturally done on cadavers of old donors.

Although the muscles chosen were from donors with no known pathology affecting limb muscle macro-vasculature or innervation, hidden adverse pathologies cannot be excluded. A possible example for such an event was muscle D in Figure 2, where the apparent lack of the main branch of the LCFA could be explained by its deterioration after blockage.

That the study derived muscle depth information for the model from a separate set of vasti than those dissected for neuro-vasculature is another study weakness. This was necessary because the study was initiated before we had the capability to generate 3D models from isolated muscles. However, we are confident that the 18 vasti from which depth maps were generated are comparable to the 28 that were

dissected. The muscles were from similar cohorts in terms of demographics, appearance and average length (36.8±2.8 cm for the dissected muscles vs 37.5±3.2 cm for the muscles used for muscle depth modelling).

Despite of these obvious limitations, the predictions from the model fit the published data on biopsy complications well. The model should have its use for the prediction of suitable biopsy sites in vastus lateralis but is not suitable for precise quantitative predictions of neurovascular parameters.

Perspectives

The neurovascular density model presented here allows for a more informed choice of biopsy sites in human vastus lateralis muscle. This will be especially important for studies involving serial biopsies (3 or more). Here a balance has to be struck between obtaining biopsies from sites separated by 3-4 cm to avoid interference from the processes involved in damage/repair affecting neighbouring biopsy sites and using a site in an area with greater neurovascular density which will carry an increased risk of complication (and have a higher chance of uneven distribution of muscle and connective tissue in a region with larger septa).

Data obtained in human vastus lateralis biopsy studies normally show significant inter-individual variability. The inter-individual variability in the intra-muscular neurovascular supply reported in this study was larger than expected on the basis of experience with biopsy studies. The results of our study should therefore be useful for the interpretation and design of experiments that involve the macro-aspects of the vastus lateralis neuro-vasculature, such as NMR blood flow or electrostimulation studies.

References

1. Tarnopolsky MA, Pearce E, Smith K, Lach B. Suction-modified Bergström muscle biopsy technique: Experience with 13,500 procedures. Muscle and Nerve 2011;43:717–725.

2. Bergström J. Muscle electrolytes in man. Scand J Clin Lab Invest 1962;14:511–513.

3. Shanely RA, Zwetsloot KA, Triplett NT, Meaney MP, Farris GE, Nieman DC. Human Skeletal Muscle Biopsy Procedures Using the Modified Bergström Technique. J Vis Exp 2014;1–8.

4. Melendez MM, Vosswinkel JA, Shapiro MJ, Gelato MC, Mynarcik D, Gavi S, Xu X, McNurlan M. Wall Suction Applied to Needle Muscle Biopsy-A Novel Technique for Increasing Sample Size. J Surg Res 2007;142:301–303.

5. Magistris MR, Kohler A, Pizzolato G, Morris MA, Baroffio A, Bernheim L, Bader CR. Needle muscle biopsy in the investigation of neuromuscular disorders. Muscle and Nerve 1998;21:194–200.

6. Phillips, Bethan E. Atherton PJVK, Limb MC, Williams JP, Smith K. No TitleAcute cocoa flavanol supplementation improves muscle macro- and microvascular but not anabolic responses to amino acids in older men. Appl Physiol Nutr Metab 2016;41:548–556.

7. Dorph C, Nennesmo I, Lundberg I. Percutaneous Conchotome Muscle Biopsy. A Useful Diagnostic and Assessment Tool. J Rheumatol 2001;28:1591–1599.

8. Highstead RG, Tipton KD, Creson DL, Wolfe RR, Ferrando A a. Incidence of associated events during the performance of invasive procedures in healthy human volunteers. J Appl Physiol 2005;98:1202–1206.

9. Willan PL, Ransome JA, Mahon M. Variability in human quadriceps muscles: quantitative study and review of clinical literature. Clin Anat 2002;15:116–128.

10.   Wolff KD, Grundmann A. The Free Vastus Laterlis Flap: An Anatomic Study with Case

Reports. Plast Reconstr Surg 1992;89:469–745.

11.   Becker I, Baxter GD, Woodley SJ. The vastus lateralis muscle: An anatomical investigation.

Clin Anat 2010;23:575–585.

12.   Willan PL, Mahon M, Golland JA, Willan PL. Morphological variations of the human vastus

lateralis muscle. J Anat 1990;168:235–239.

13.   Wang Y, Begue T, Masquelet A. Anatomic Study of the Distally Based Vastus Lateralis

Muscle Flap. Plast Reconstr Surg 1999;103:101–103.

14.   Grob K, Monahan R, Gilbey H, Ackland T, Kuster MS. Limitations of the Vastus Lateralis

Muscle as a Substitute for Lost Abductor Muscle Function: An Anatomical Study. J

Arthroplasty 2015;30:2338–2342.

15.   Darpa S, Toia F, Brenner E, Melloni C, Moschella F, Cordova A. Variability and reliability of

the vastus lateralis muscle anatomy. Acta Chir Belg 2016;116:203–212.

16.   Grob K, Manestar M, Lang A, Ackland T, Gilbey H, Kuster MS. Effects of ligation of lateral

intermuscular septum perforating vessels on blood supply to the femur. Injury 2015;46:2461–

2467.

17.   Revenaugh PC, Knott PD, McBride JM, Fritz MA. Motor nerve to the vastus lateralis. Arch

Facial Plast Surg 2012;14:365–368.

18.   Schindelin J, Arganda-Carreras I, Frise E, Kaynig V, Longair M, Pietzsch T, Preibisch S,

Rueden C, Saalfeld S, Schmid B, Tinevez JY, White DJ, Hartenstein V, Eliceiri K, Tomancak

P, Cardona A. Fiji: An open-source platform for biological-image analysis. Nat Methods

2012;9:676–682.

19.   Kendall DG. A Survey of the Statistical Theory of Shape. Stat Sci 1989;4:87–99.

20.   Rueckert D, Sonoda L, Hayes C, Hill D, Leach M, Hawkes D. Nonrigid registration using free-form deformations: application to breast MR images. Med Imaging, IEEE Trans 1999;18:712–721.

21.   Wu C. Towards Linear-time Incremental Structure from Motion. 3DTV-Conference, 2013 Int Conf 2013;127–134.

22.   Wu C. VisualSFM : A Visual Structure from Motion System.

23.   Cignoni P, Cignoni P, Callieri M, Callieri M, Corsini M, Corsini M, Dellepiane M, Dellepiane M, Ganovelli F, Ganovelli F, Ranzuglia G, Ranzuglia G. MeshLab: an Open-Source Mesh Processing Tool. Sixth Eurographics Ital Chapter Conf 2008;129–136.

24.   Flato R, Passanante GJ, Skalski MR, Patel DB, White EA, Matcuk GR. The iliotibial tract: imaging, anatomy, injuries, and other pathology. Skeletal Radiol 2017;46:605–622.

25.   Patel, Harnish P; Cooper, Cyrus; Sayer AA. 2012. Percutaneous Muscle Biopsy: History, Methods and Acceptability. In: Sundaram C, ed. Muscle Biopsy. Rijeka: InTech, 1–14.

26.   Hennessey J V, Chromiak J a, Della Ventura S, Guertin J, MacLean DB. Increase in percutaneous muscle biopsy yield with a suction-enhancement technique. J Appl Physiol 1997;82:1739–42.

27.   Neves M, Barreto G, Boobis L, Harris R, Roschel H, Tricoli V, Ugrinowitsch C, Negrão C, Gualano B. Incidence of adverse events associated with percutaneous muscular biopsy among healthy and diseased subjects. Scand J Med Sci Sport 2012;22:175–178.

28.   Heckmatt JZ, Moosa A, Hutson C, Maunder-Sewry CA, Dubowitz V. Diagnostic needle muscle biopsy. Arch Dis Child 1984;59:528–532.

29.   Edwards RH, Round JM, Jones DA. Needle biopsy of skeletal muscle: a review of 10 years experience. Muscle Nerve 1983;6:676–683.

30. Evans WJ., Coggan AR. Muscle Biopsy as a Tool in the Study of Aging. Journals Gerontol Ser A 1995;50A:30–34.

31. Gibala MJ, Maclean DA, Graham TE, Saltin B, MacLean DA, Gra-ham TE. Tricarboxylic acid cycle intermediate pool size and estimated cycle flux in human muscle during exercise. AJP Endocrinol Metab 1998;275:E235-242.

32. Hanasono, Matthew M. M.D.; Skoracki, Roman J. M.D.; Yu PMD. A Prospective Study of Donor-Site Morbidity after Anterolateral Thigh Fasciocutaneous and Myocutaneous Free Flap Harvest in 220 Patients. Plast Reconstr Surg 2010;125:209–214.

33. Boman N, Burén J, Antti H, Svensson MB. Gene expression and fiber type variations in repeated vastus lateralis biopsies. Muscle and Nerve 2015;52:812–817.

34. Kimata Y, Uchiyama K, Satoshi E, Nakatsuka T, Kiyonoki H. Anatomic Variations and Technical Problems of the Anterlolateral Thigh Flap: A Report of 74 Cases. Plast Reconstr Surg 1998;102:1517–1523.

35. Bearden SE. Effect of aging on the structure and function of skeletal muscle microvascular networks. Microcirculation 2006;13:279–288.

Acknowledgements

Figure legends

Figure 1: Generation of vessel traces. A) The vessels and nerves were dissected as far as possible within the vastus lateralis. B) In order to improve their visibility, they were painted with nail polish (red for arteries, blue for veins and green for nerves).

A transparency was fastened over the muscle with pins and the painted vessels and nerves traced with felt tipped pens. The transparency with the traces was then scanned to obtain a digital image (C). Note a transverse branch of the lateral circumflex femoral artery in A) with its flow direction indicated by an arrow and two apposed venae comitantes (arrowheads).

Figure 2: Representative traces from eight vasti laterales showing the dissected arteries in red, veins in blue, nerves in green and the muscle bellies' circumference with a fine black line.

The figure illustrates the inter-individual variability of the intra-muscular neurovascular structures.

The main blood supply was from and to branches of the lateral circumflex femoral artery (LCFA) and vein (LCFV) (arrowheads ①), respectively, with variable contributions from branches originating from the deep femoral artery and vein (arrowheads ②). In some muscles, anastomoses between the two could be dissected (arrowheads ③). ④ indicates vessels joining the vastus lateralis from deep through the vastus intermedius. Vessels ⑤ entered it from the femur's surface. ⑥ indicates a nerve entering the vastus lateralis from the underlying vastus intermedius.

Figure 3 shows the estimated volume density of dissectable arteries, veins and nerves plus all of them combined, modelled by incorporating the 2D-maps shown in Supporting Figure S2 with the volumetric information of the average vastus lateralis shown in Supporting Figure S3. Only the intra-muscular neuro-vasculature is shown.

The mean shape of the circumference is shown as red contour. The colour scale has been adjusted to represent the probability of a cylinder with 4 mm diameter and 15 mm length contacting one of the mapped structures, as an approximation of a 200 mg biopsy obtained with a Bergström needle with

25

suction.

Just posterior to a proximal-distal midline, there is a zone of lower density of vessels and nerves. The volume density of veins and arteries is higher along the posterior margin, representing the contributions from the deep femoral artery and vein.

The area with the lowest combined density is indicated by a white line, but in the thigh, it is mostly covered by the iliotibial tract, as indicated in Figure 4 and Supporting Figures 8 and 9.

Figure 4: Screenshots from the vessel/nerve distribution model projected onto the 3D surface of an *in situ* vastus lateralis. 3D-pdf files of the corresponding models are shown in the supporting information (Supporting Figures S8 and S9).

A) Shows the volume density of vessels and nerves combined adapted onto the 3D vastus lateralis surface.

Light green indicates a projection of the iliotibial band, including the tensor fasciae latae tendon, onto this surface. The red line connects the greater trochanter with the lateral base of the patella.

The area with the lowest density indicated in Figure 3 is again outlined in white. It is covered by the projection of the iliotibial tract. From the middle of the muscle on distally, there is a band of low neurovascular density just anterior to the iliotibial band that stretches to about ¾ of the muscle's distance between the greater trochanter and the lateral epicondyle. This is the zone most suitable for a needle biopsy according to our model.

B) shows a similar screenshot to A with needle biopsy sites recommended in the literature indicated.

Brown marks the recommendation of [4] and [2] "approximately 15 cm from the lateral superior border of the patella".

Purple shows the zone mentioned in [1] and [3] "just anterior to the lateral fascia (iliotibial tract), between 25% and 50% of the distance from the lateral joint line to the greater trochanter".

Pink points to the region in [25] "approximately two-thirds down a line from the anterior superior iliac spine to the patella".

Dark green indicates the zone of [26] and [27] "25 cm proximal from the tuberositas tibiae and 5 cm lateral from the midline of the femoral course".

The recommendations in [1] and [3] are the best fit to the suitable low density area in our model. These studies also had the lowest complication rates in our comparison (table 3).

Position markers were placed in the thigh, on the top of the greater trochanter and the lateral epicondyle (blue painted screws) as well as the anterior superior iliac spine and the middle of the patella (cyan painted screws). They were used to scale and orient the 3D reconstruction.

27
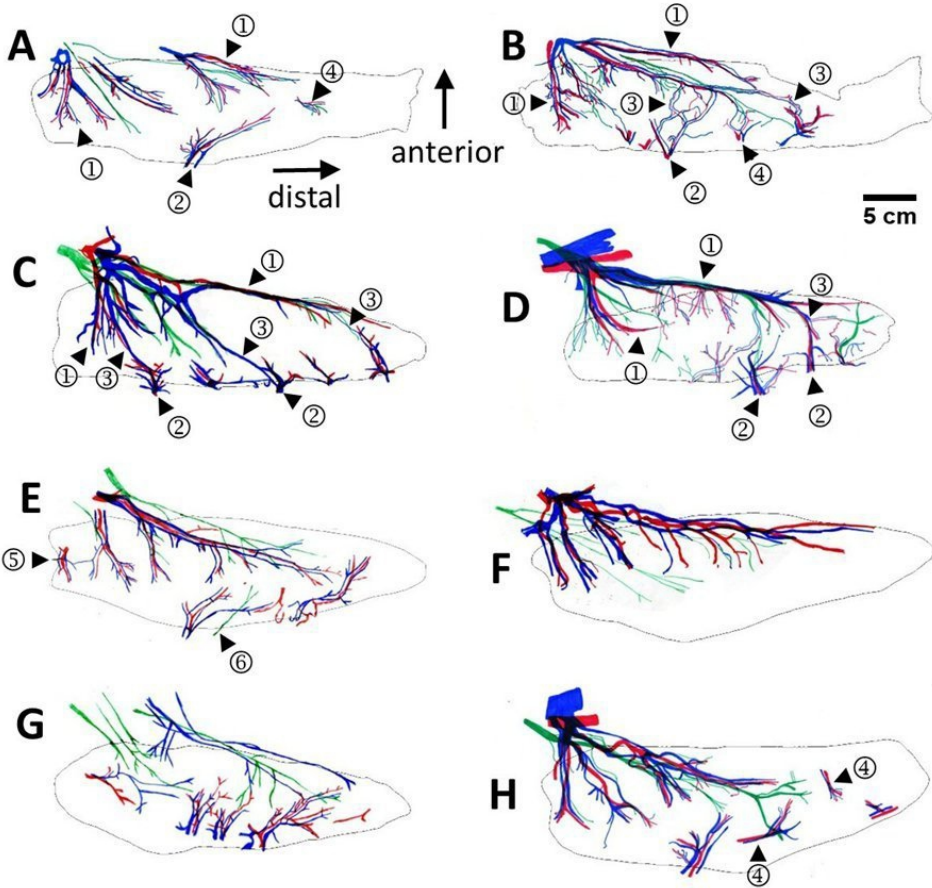
Figure 1: generation of tracings

311x91mm (72 x 72 DPI)
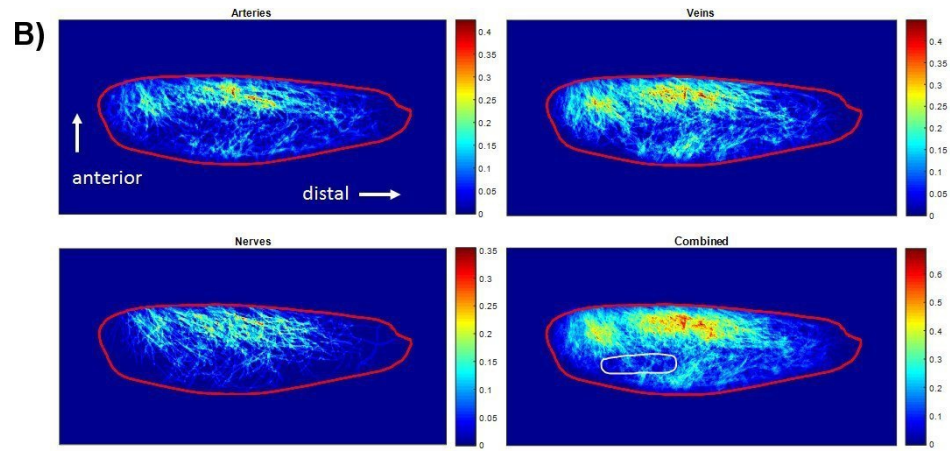
Figure 2: Representative tracings

331x335mm (72 x 72 DPI)

Figure 3: Volume density of all vasti combined
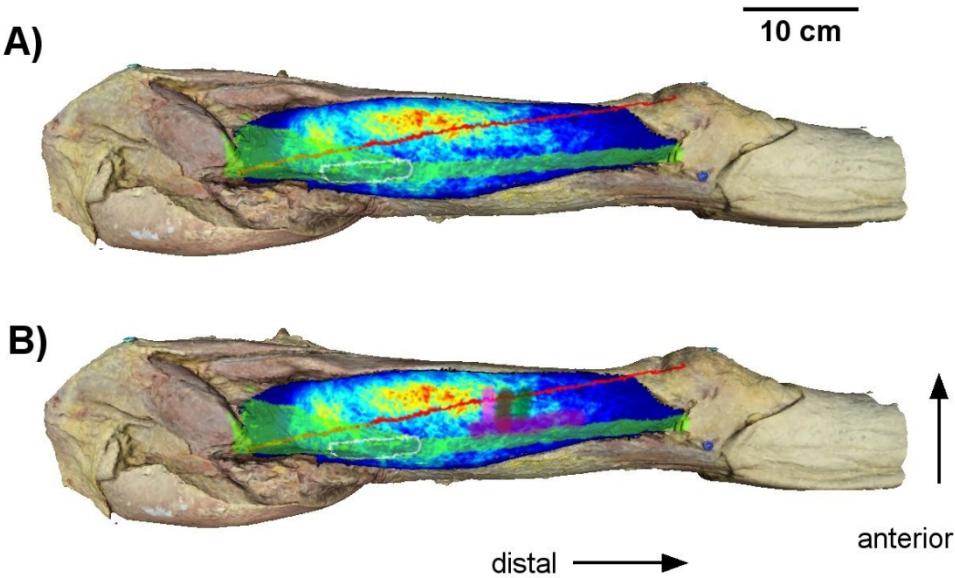
402x218mm (72 x 72 DPI)

1
2
3
4
5
6
7
8
9
10
11
12
13
14
15
16
17
18
19
20
21
22
23
24
25
26
27
28
29
30
31
32
33
34
35
36
37
38
39
40
41
42
43
44
45
46
47
48
49
50
51
52
53
54
55
56
57
58
59
60

Figure 4: Screenshots of density model on 3D thigh

437x296mm (72 x 72 DPI)

Table 1

	Mean of all vasti laterales ± S.D.	Mean of female vasti laterales ± S.D.	Mean male vasti laterales ± S.D.	t-test on difference female - male
Distance between greater trochanter and lateral aspect of patellar base (cm)	36.8 ± 2.8	35.1 ± 3.7	37.9 ± 1.7	p<0.05
Length of dissected muscle belly (cm)	34.41 ± 2.8	32.8 ± 3.2	35.5 ± 2.0	p<0.05
Combined length of dissected arteries (cm)	77.1 ± 26.5	60.7 ± 22.0	87.8 ± 23.9	p<0.05
Combined length of dissected veins (cm)	113.1 ± 37.6	94.5 ± 32.7	125.1 ± 36.3	p<0.05
Combined length of dissected nerves (cm)	61.4 ± 27.3	46.7 ± 10.4	70.8 ± 30.8	p<0.05
Proportion of arteries accompanied by veins (%)	80.6 ± 10.9	85.6 ± 8.4	77.4 ± 11.3	p<0.05
Proportion of nerves neighbouring a vessel (%)	66.9 ± 11.0	66.4 ± 10.9	67.2 ± 11.3	N.S.
Proportion of arteries from branches of the LCFA (%)	74.0 ± 18.7	75.8 ± 15.7	72.8 ± 20.8	N.S.
Proportion of veins to branches of the LCFV (%)	72.1 ± 16.7	69.7 ± 17.0	75.6 ± 16.9	N.S.

Table 1: Length measurements of vastus lateralis muscles and the dissected arteries, veins and nerves. The vessel/nerve data are derived from the intra-muscular portions of the dissected neuro-vasculature, defined by the circumference of the muscles in the tracings.
S.D.: Standard deviation. N. S: not significant at the 0.05 level.

Table 2:

Literature source	Biopsy site description	Colour in Figure 4B and Supporting Figure S9
1	"just anterior to the lateral fascia (iliotibial band), between 25% and 50% of the distance from the lateral joint line to the greater trochanter"	purple
3	the same as in [1]	purple
2	"15-20 cm above the knee"	brown
4	"lateral mid-thigh at approximately 15 cm from the superior border of the patella"	brown
25	"approximately two-thirds down a line from the anterior superior iliac spine to the patella"	pink
26	"at a point 25 cm proximal from the tuberositas tibiae and 5 cm lateral from the midline of the femoral course"	dark green
27	The same as in [26]	dark green

Table 2: Recommended biopsy sites as described in the literature. Their approximate location is indicated by the different colours in Figure 4B and Supporting Figure S9.

Table 3:

literature source	Needle	Number of biopsies in total	Bleeds (arterial, haematomas, erythema, ecchymosis)	Skin infections	Localised numbness / pain > 3 days	Rate of complications per biopsy
[29]	Bergström or equivalent	400	3			0.75%
[26]	Bergström or equivalent	83	1		1	2.4%
[8]	Bergström or equivalent	1288	20			1.55%
[1]	Bergström or equivalent	13914	4	8	5	0.16%
[27]	Bergström or equivalent	496	14		6	4%
[3]	Bergström or equivalent	1600		2		0.13%
[5]	Micro-Needle	198	2			1.01%

Table 3: Incidence rates and type of complications for vastus lateralis needle biopsies from eight different studies. Where an exact description of the biopsy site was available, it is indicated in Figure 4 B and Supporting Figure S9.
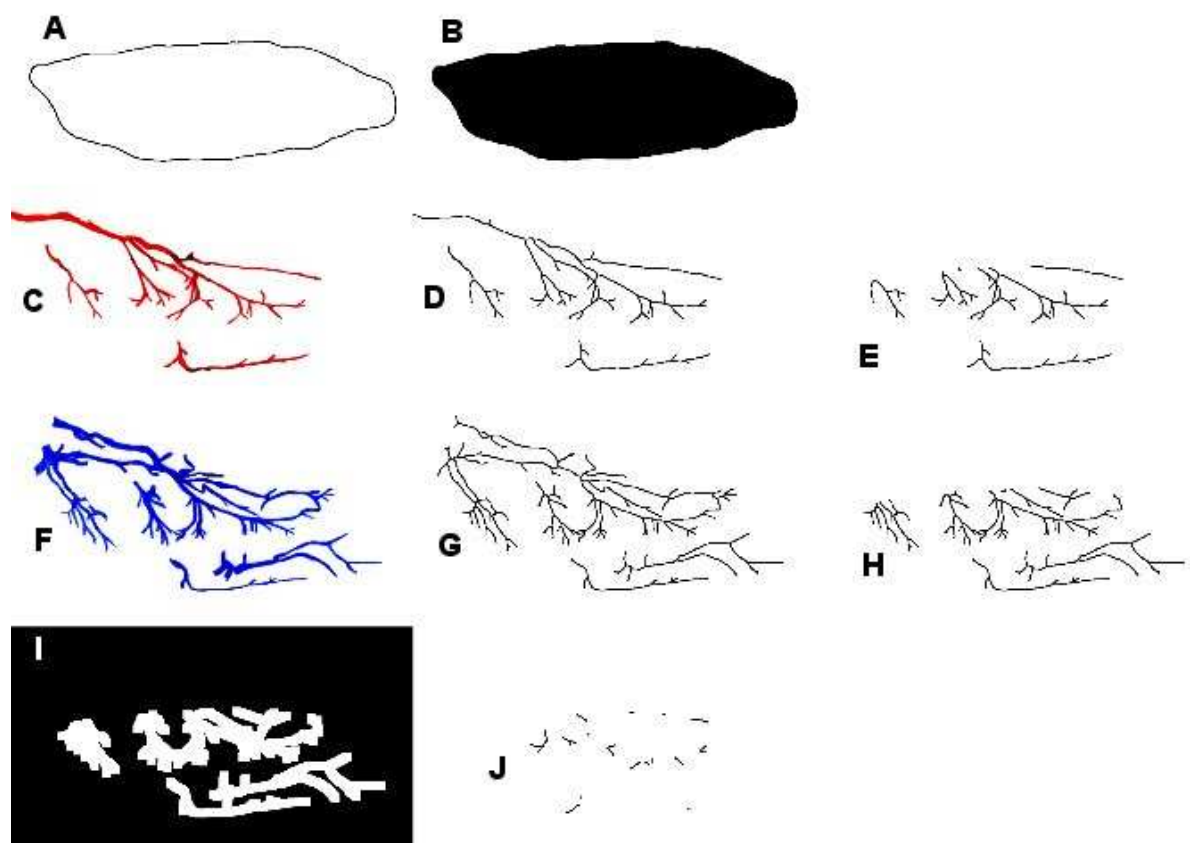
Supporting Figure S1: Estimate of vessel tree length and the proportion of arteries covered by veins using imageJ. A black shape (B) was generated from the skeletonised muscle circumference (A). The arterial trace (C) and venous trace (F) were reduced to a skeleton of 1-pixel width (D, G). The union of B and D (by adding B and D in imageJ's image calculator) resulted in restriction of the arterial tree to the intra-muscular portion (E), because in binary images, a black pixel has a grey value of zero and a white pixel of 255. Correspondingly, the intra-muscular portion of skeletonised veins (H) was generated by calculating the union of B and G. To display the portion of arteries not neighbouring a vein, the intra-muscular venous skeleton was enlarged to 6 mm width and inverted to white on black background (I). This was then added to the skeletonised intra-muscular arteries (E) to yield the stretches of arteries (J) not associated with veins, here defined as further than 3 mm away from the middle of a vein trace.
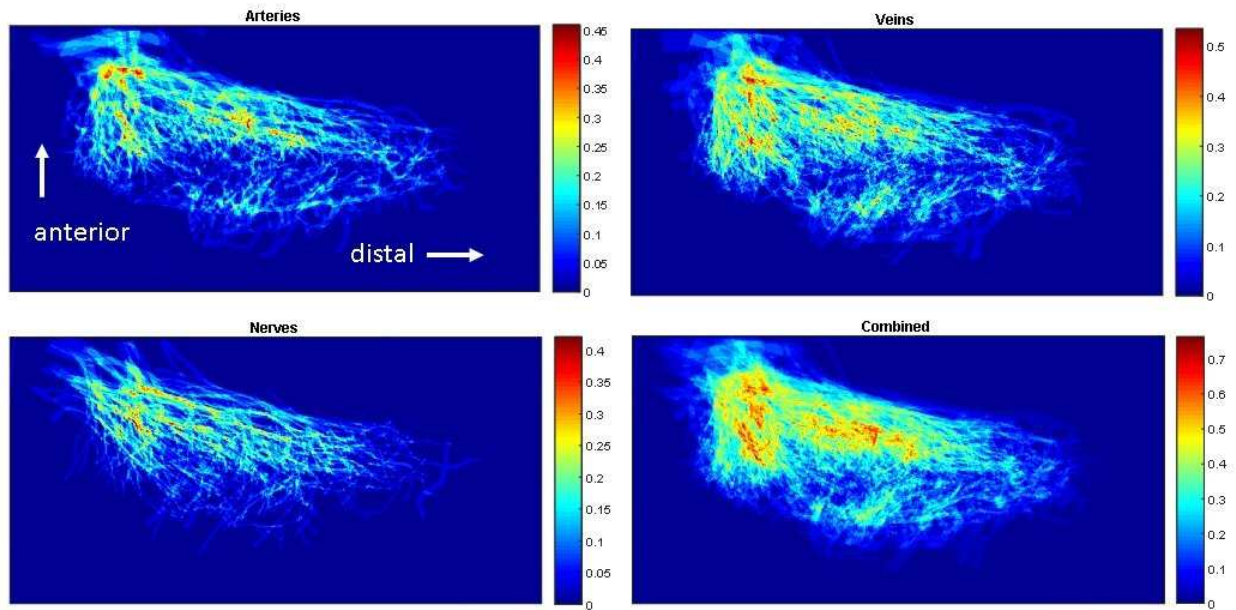
Supporting Figure S2: Superimposition of the 28 artery, vein and nerve traces after their adjustment to a reference coordinate. The colour scale on the right-hand side indicates density.

A zone of lower vessel and nerve density is visible just posterior to a proximal-distal midline. Veins and arteries have a zone of higher density along the posterior margin, representing the contributions from the deep femoral artery and vein.

Since these densities are derived from adjusted 2D tracings, they do not take muscle depth into account. The combination of these 2D density maps with the depth information in the 3D average vastus lateralis from the second cohort (Supporting Figure S3) yielded the volume density model shown in Figure 3 of the paper.
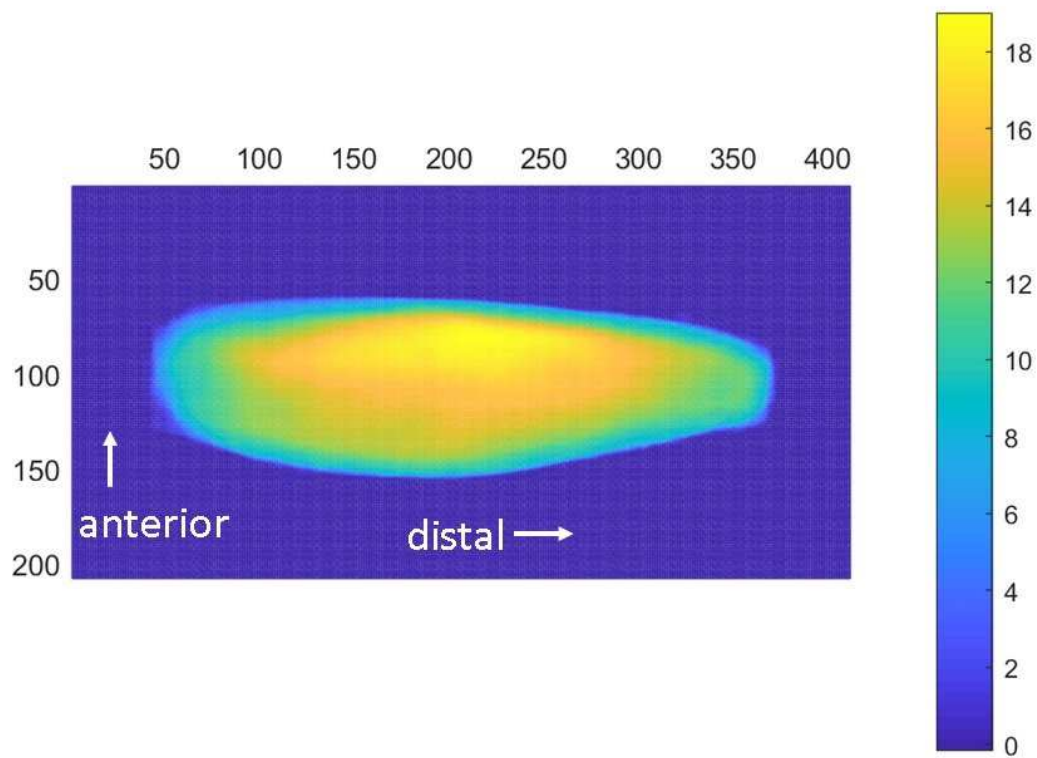
Supporting Figure S3: 3D average of the flat lying vastus lateralis muscles from all 18 donors in the second cohort, shown as height map.

Combining the depth information shown in this figure with the 2D density maps in Supporting Figure S2 resulted in the volumetric density map shown in Figure 3 of the paper.

Numbers indicate mm, colour represents Z-distance from bottom to surface of the muscle, in mm.
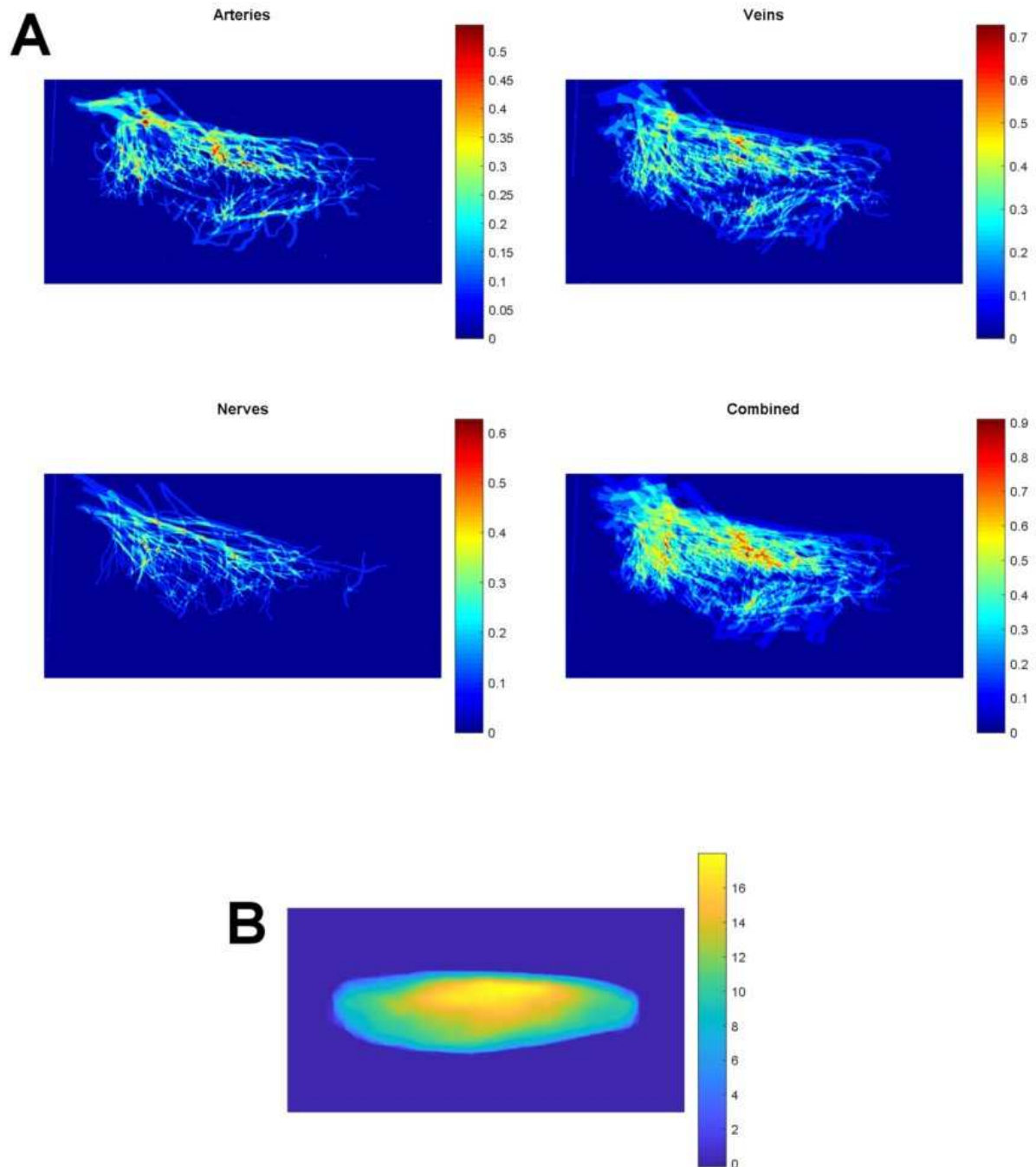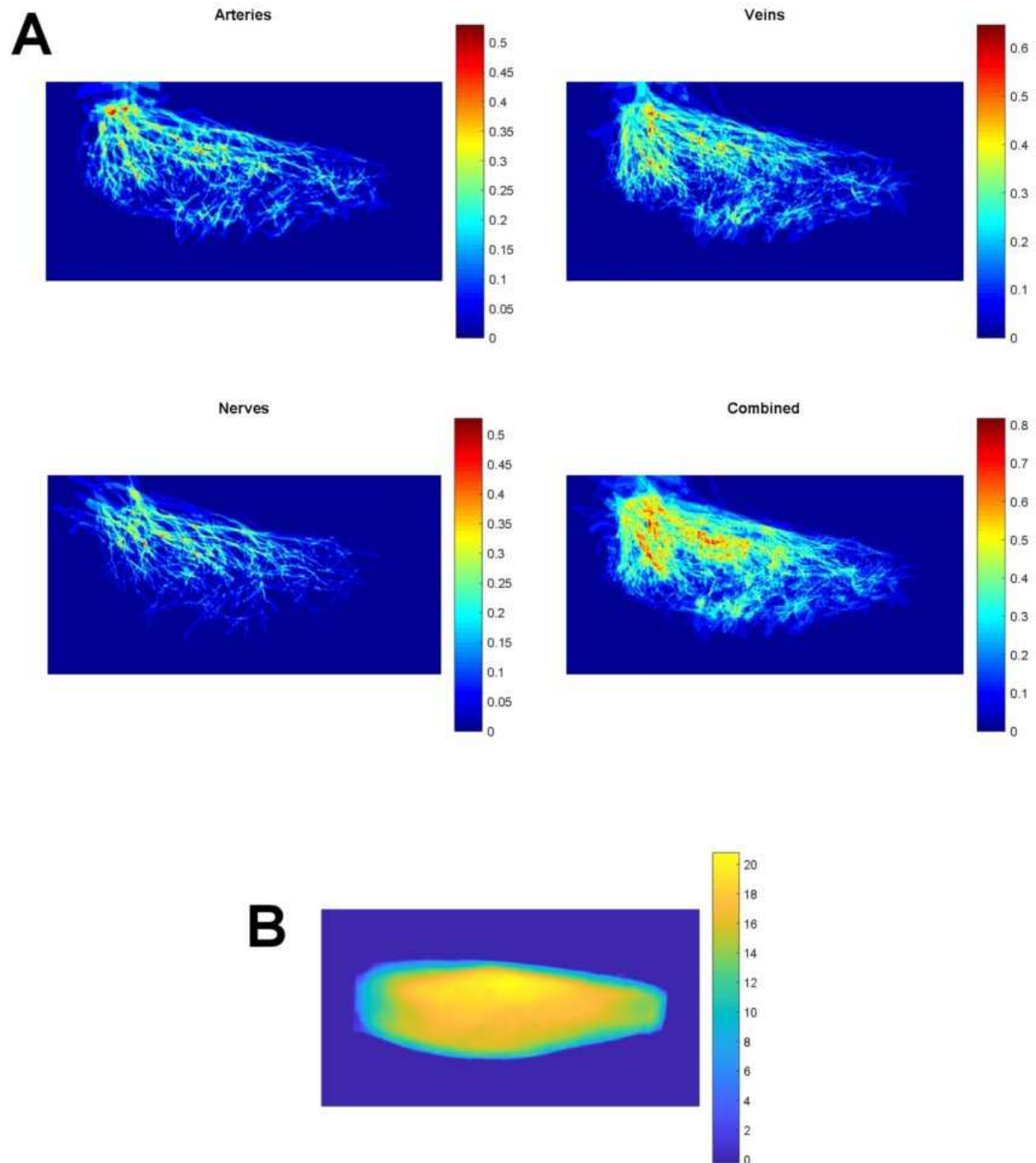
Supporting Figure S4: A) Superimposition of the artery, vein and nerve traces from the 11 female vasti after their adjustment to a reference coordinate. The colour scale on the right-hand side indicates density.

There are no obvious differences in the patterns of superimposed traces between these female muscles and the male muscles shown in Supporting Figure S5.

B) 3D average of the flat lying vastus lateralis muscles from the 8 females in the second cohort, shown as height map. The colour scale indicates height in mm. As expected, the maximum height was lower (17.99mm) than the averaged male muscles (21.78 mm, Supporting Figure S5).

Combination of the 2D density maps in A) with the height map in B) resulted in the volume density maps for the female muscles shown in Supporting Figure S6.

Supporting Figure S5: A) Superimposition of the artery, vein and nerve traces from the 17 male vasti after their adjustment to a reference coordinate. The colour scale on the right-hand side indicates density.
There are no obvious differences to the female vastus patterns shown in Supporting Figure S4.
B) 3D average of the vastus lateralis muscles from the 10 males in the second cohort shown as height map. The colour scale indicates height in mm. The maximum height (21.78 mm) was higher than in the female muscle average (17.99 mm, Supporting Figure S4).
Combination of the 2D density maps in A) with the height map in B) resulted in the volume density maps for the male muscles shown in Supporting Figure S7.
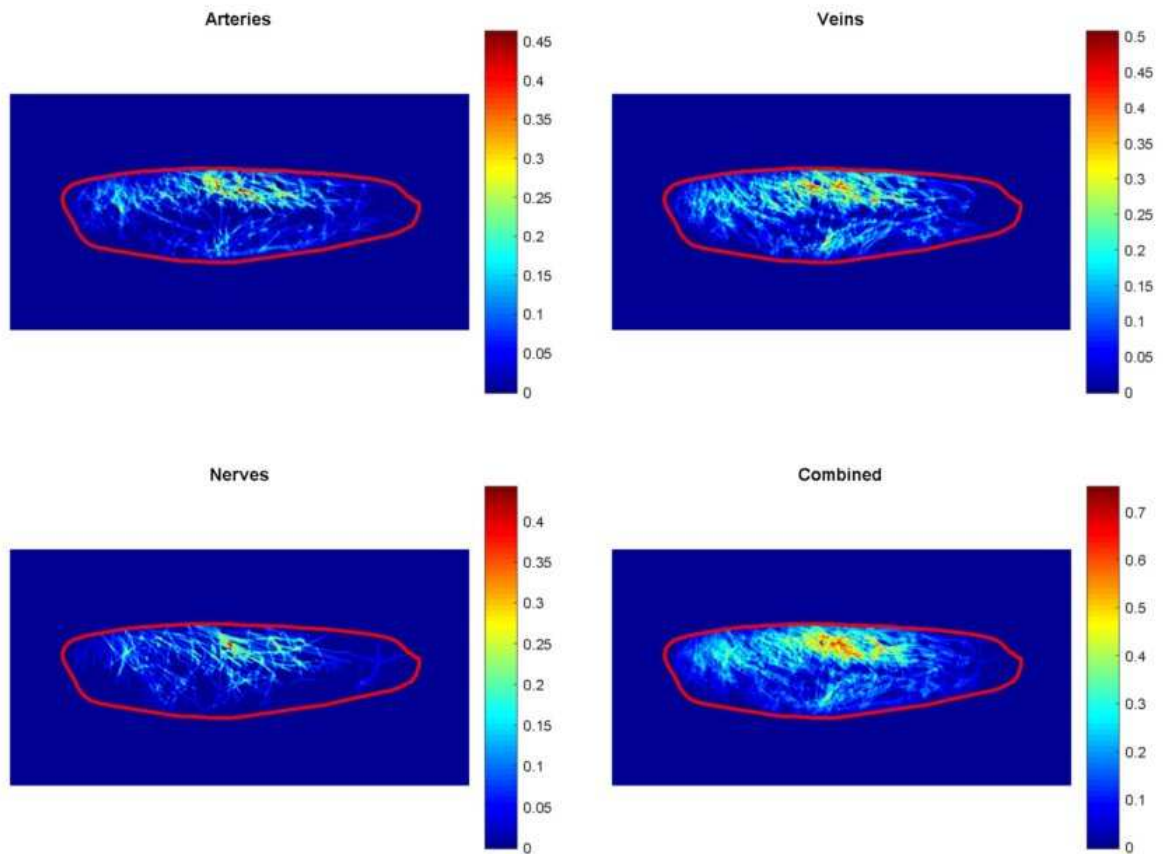
Supporting Figure S6: Volume density of dissectable arteries, veins and nerves in the vasti from the 11 female donors. The colour scale on the right-hand side indicates density corrected for depth. The mean shape of the circumferences is shown as red contour.

After taking into account the lower density due to fewer muscles in the female graphs, no obvious differences were apparent between the maps of females and males (Supporting Figure S7).
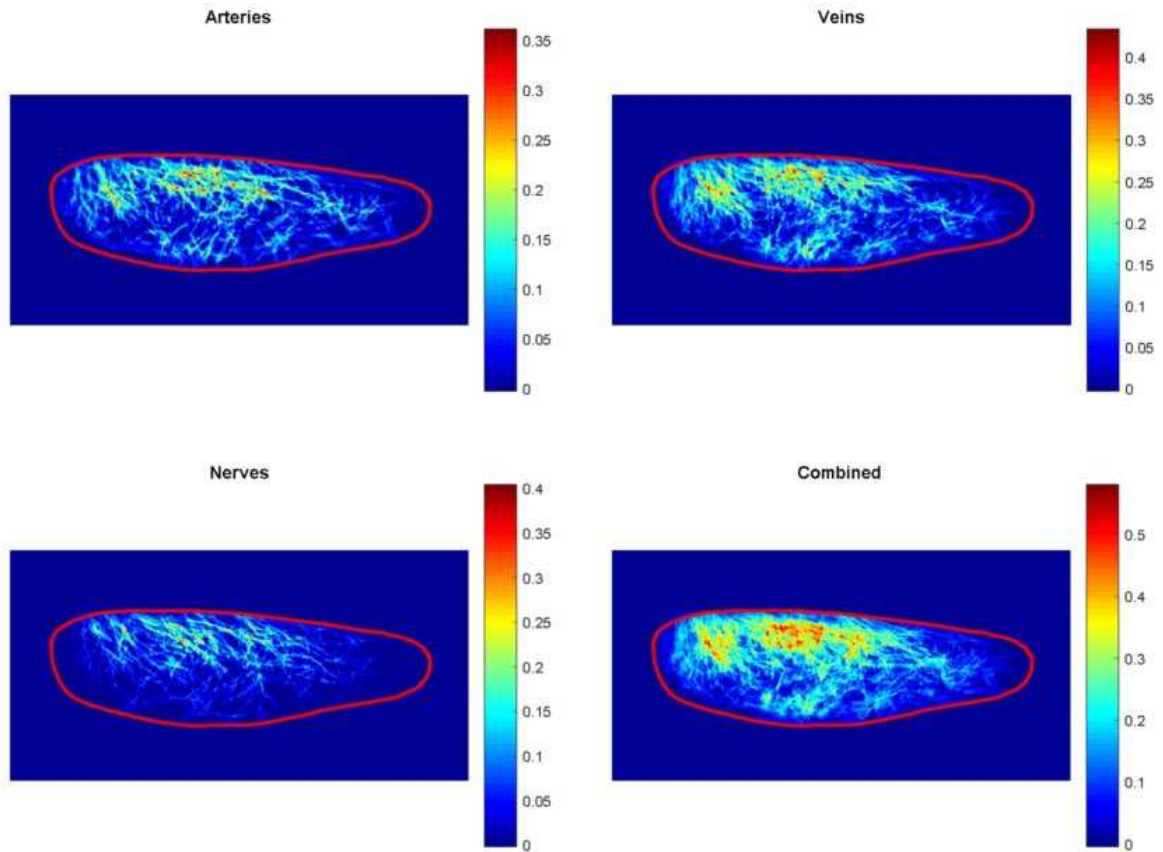
Supporting Figure S7: Volume density of dissectable arteries, veins and nerves in the vasti from the 17 male donors. The colour scale on the right-hand side indicates density corrected for depth. The mean shape of the circumferences is shown as red contour.

We could not detect any systematic differences between the volume density maps of female (Supporting Figure S6) and male muscles (this figure).

(figureS8.u3d)

Supporting figure S8: 3D model corresponding to figure 4 A in the paper.
It shows the combined vessel/nerve volume densities shown in figure 3 of the
paper adapted to the 3D surface of a vastus lateralis from a 78 year old male
donor.
Clicking on (figureS8.u3d) will load the model. Holding the left mouse button
down while moving the mouse changes the camera position. Pressing ctrl while
turning the mouse wheel allows zooming.
Light green indicates a projection of the iliotibial band, including the tensor
fasciae latae tendon onto this surface. A red line has been drawn between the
major trochanter and the lateral base of the patella.
The area with the lowest densities shown in figure 3 is indicated by a white line.
It is covered by the iliotibial tract and therefore not suited as access site for a
needle biopsy. Distal to the middle of the muscle is a band of low neurovascular
density just anterior to the iliotibial band that stretches to about three quarters
of the distance from the major trochanter to the lateral epicondyle. This is the
zone most suitable for a needle biopsy according to our model.
Position markers (blue or cyan painted screws) were placed on the top of the
trochanter major, lateral epicondyle, anterior superior iliac spine and the middle
of the patella. They were used to scale and orient the 3D reconstruction.

(figureS9.u3d)

Supporting figure S9: 3D model corresponding to figure 4 B in the paper. It shows the same vessel/nerve distribution model adapted to the in situ vastus lateralis as shown in figure 4 A/supporting figure S8 with the recommended needle biopsy sites from table 2.

Clicking on (figureS9.u3d) will load the model. Holding the left mouse button down while moving the mouse changes the camera position Pressing ctrl while turning the mouse wheel allows zooming.

Brown indicates the recommendation in [2] and [4]: "approximately 15 cm from the lateral superior border of the patella".

Purple shows the zone mentioned in [1]: "just anterior to the fascia lata (iliotibial tract), between 25% and 50% of the distance from the lateral joint line to the greater trochanter", which corresponds to [3].

Pink points to the biopsy region in [25]: "approximately two-thirds down a line from the anterior superior iliac spine to the patella".

Dark green indicates the zone in [26] and [27]: "25 cm proximal from the tuberositas tibiae and 5 cm lateral from the midline of the femoral course".

The recommendations in [1] and [3] are the best fit to the suitable low density area in our model. Both studies also had the lowest complication rates in our comparison (table 3 in the paper).